



## A Novel Method Based on Interpolation for Accurate 3D Reconstruction from CT Images

**Waad Q. Shiaa<sup>1\*</sup>****Amjad B. Abdulghafour<sup>1</sup>****Omar H. Hassoon<sup>1</sup>**

<sup>1</sup>*Department of Production Engineering and Metallurgy, University of Technology - Iraq, Baghdad, Iraq*

\* Corresponding author's Email: [waad.q.shiaa@uotechnology.edu.iq](mailto:waad.q.shiaa@uotechnology.edu.iq)

---

**Abstract:** In intervention procedures or planning for joint replacement, the models developed must be precise and represent the natural look of the bones. For instance, the function of the knee joint is dependent on the motion of the femur. Therefore, precisely reconstructing the femur model assists in the design of the components for joint replacement. Moreover, when accurate measurements are taken for implant design, these models have a high effect on their accuracy. As a result, obtaining accurate 3D models of human bone tissue is important. Therefore, this paper proposes a novel method for accurate bone tissue reconstruction from CT data. The method is based on histogram modelling, interpolation, and reverse engineering techniques. Initially, soft tissues and unwanted artifacts are eliminated in order to extract the ROI (bone). After that, feature points are extracted based on pixel variance from each slice and then interpolated to create a 3D point cloud. Finally, a 3D model is created from point cloud data. Additionally, the model is printed using a 3D printer based on the FDM technique. Furthermore, the method is tested on CT stacks of femur and sheep bone in order to evaluate its strength and performance. Results indicated that the feature points collected by the proposed method could accurately describe the bone geometry. The error percentage between the proposed method and the actual bone was approximately 1.62%. The results indicate that the proposed method provides promising outcomes. Furthermore, the 3D model of bone is more compatible with the real bone.

**Keywords:** CT images, Image segmentation, Interpolation, Reverse engineering, 3D reconstruction, 3D printing.

---

### 1. Introduction

Medical imaging methods such as computed tomography (CT) and magnetic resonance imaging (MRI) have experienced significant advancements in recent years. These techniques are now widely employed in medicine, sciences, and engineering to analyze the interior architecture of a wide range of tissues and organs. The emergence of MRI and CT scans for X-rays made it possible for researchers and medical staff to see the human body's interior anatomical features in three-dimensional (3D). This allowed physicians and researchers to create 3D computer models of human anatomy and conduct studies that would have been impossible to try on real people. Consequently, 3D reconstruction of anatomical features from CT and MRI images became a key research focus. CT and MRI are the standard imaging modalities used to explore bones

and organs. While MRI is an accurate, radiation-free imaging method for studying soft tissues, CT is preferable for investigating bone structures [1, 2].

Recently, 3D models' reconstruction of human organs using CT imaging has become more important in a variety of medical fields. The 3D models can provide surgeons with access to important medical information. It may also be used to create prostheses, implantations, and tissue scaffolding, in addition to performing a variety of simulation and analytical tasks. Besides that, bone surgery needs a 3D model of a patient's bone to plan the surgery and design specialized implants [3]. A bone has two different regions: cortical and cancellous tissues. The exterior layer of a bone is made up of cortical tissue, which is exceedingly bushy. Cancellous tissue is found primarily at the ends of the bones (joint regions), is more variable, and has a lower density on CT images

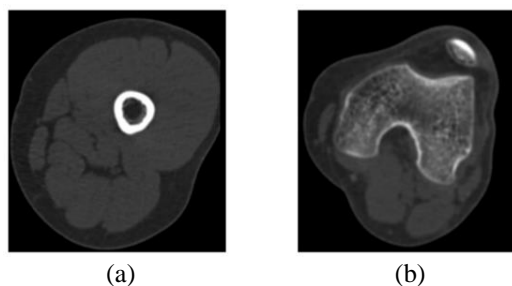


Figure. 1 CT images of the same person: (a) Cortical tissue and (b) Cancellous tissue

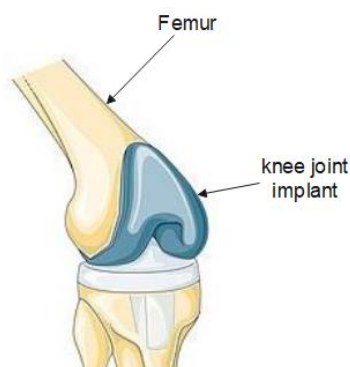


Figure. 2 Schematic of a knee joint replacement.

[4]. Furthermore, the intensity values of both tissues may not be similar throughout all images. Fig. 1 illustrates the intensity variance of tissues within a CT stack of the same person. To produce 3D models, CT images must often be processed to obtain the bone's structure and then converted into the models. In general, the total accuracy of a 3D model rebuild strictly depends on (i) the quality of the patient imaging data, (ii) the image segmentation step, and (iii) the reconstruction technique. Each of these steps is critical in establishing the precision of the 3D model's geometry. However, image segmentation is one of the most critical and complex stages, making it more prone to mistakes than others. Consequently, it is not easy to reconstruct bone tissues from surrounding artifacts and to generate accurate 3D models from CT images.

In intervention procedures or planning for joint replacement, the models developed must be precise and represent the natural look of the bones. Additionally, the design of implants requires highly precise 3D models. For instance, the function of the knee joint is dependent on the motion of the femur. Therefore, precisely reconstructing the femur model assists in the design of the implant for knee joint replacement, as shown in Fig. 2. Furthermore, when accurate measurements are taken for implant design, these models have a high effect on their accuracy.

Several algorithms and applications are available to create these models from CT images. These algorithms and applications use various segmentation

methods. Threshold, region growth, and active contour are some examples. These methods depend on user-defined threshold values, or "seeds" to segment images. Furthermore, the intensity values of cancellous tissue in joint areas approximate those of the flesh surrounding it. As a result, accurately segmenting bones in the joint region is difficult. Thus, over- or under-segmentation occurs more frequently. Consequently, when relying on these results, models that are larger or smaller in size than the real bone will be produced. Besides, these applications create more complex models. Therefore, additional processing procedures are required to simplify it using other tools and make it suitable for implant design. Each of these procedures has an effect on the accuracy of the models. As a result, when designing an implant, such as the knee joint implant, using these models, the accuracy of the designed implant will not be high, which causes it to be ineffective.

Until now, there has been no attempt to create accurate and simple 3D models. Therefore, this paper proposes a novel method for accurately reconstructing the human bone model from CT data. The method is based on histogram modelling, interpolation, and reverse engineering techniques. Firstly, soft tissues are eliminated in order to extract the region of interest (ROI). Next, feature points are extracted and interpolated from each slice to generate a 3D point cloud. Finally, the point cloud is converted into a 3D model. Additionally, the method is tested on the bone of a sheep to evaluate its strength and performance. Furthermore, the model of the proposed method is compared to the result of open-source software (3D Slicer). During the comparison, the proposed method produced promising results.

The remainder of the paper is laid out as follows: section 2 illustrates related works. The proposed method is described in section 3. Section 4 contains the results as well as a commentary on the results. Finally, the conclusion and future work are discussed in section 5.

## 2. Related works

Several studies have been published to reconstruct 3D models from medical images in the literature, some of which are covered below.

Menaka et al. [5] applied the discrete curvelet transformation to create a 3D point cloud from CT slices. The method depended on initial thresholding to extract the ROI (bone) and curvelet transformation for feature point extraction from each slice. However, when the threshold technique is used to highlight the ROI, some feature points are lost. Chougule et al. [6] used the Sobel edge detector to create the 3D point

cloud. This method was also based on the threshold technique. However, when the Sobel method is used, points are extracted that don't represent the features of the bones. Zhang et al. [7] presented a 3D segmentation method for the mandible and maxilla based on their different structures. Initially, a Canny edge detector was used to detect edges and enhance them with a suitable threshold. Secondly, the region growth approach was employed to separate the mandible and maxilla. Finally, a morphological process was used to fill in the internal holes. However, some redundant edges remain that don't represent ROI. Furthermore, this approach is more sensitive to image noise and requires more time.

Additionally, the authors used a variety of applications to reconstruct 3D models. These applications are divided into two types: one is open-source, such as 3D Slicer (USA), and the other is commercial, like Mimics (Belgium). These tools can segment the raw images to highlight the ROI. Furthermore, the ROI can be transformed into 3D models describing the geometry of tissues and organs [8]. Osti et al. [9] explained a way to reconstruct kids' bones based on several programs. Reconstruction of a 3D model from CT slices requires InVesalius software. Then, the model was repaired and simplified using MeshLab. Finally, Blender was used to optimize the mesh. The study depended on many tools, which led to several processing methods. This will have an effect on the model's accuracy. Especially when using InVesalius to highlight ROI. Alawy and Abdulghafour [10] proposed a method for designing, manufacturing, and simulating implants based on medical imaging data. They used several programs, like 3D Slicer, Solidworks, and Meshmixer. The study relied on the manual threshold technique for segmentation of the images. However, the manual thresholding method is more time-consuming. Masilamani et al. [11] explained the procedures involved in creating a 3D model of the hip joint for analysis purposes. Used software like 3D Slicer, Meshmixer, and MeshLab to rebuild the model, repair it, and simplify it, in that order. Finally, the file was saved in the STEP/IGES format using SolidWorks. However, the method of segmentation used is not precise.

In order to evaluate the accuracy, some authors used 3D scans to compare models. Soodmand et al. [12] offered a deviation analysis to assess segmentation methods based on CT imaging versus 3D scans of the same bone. The femur was segmented using four diverse software programs: AMIRA, Mimics, YaDiv, and Fiji-Medtool, by experts with different skills. The results indicate that the average deviation of rebuilt models was about 0.79 mm.

Puggelli et al. [13] studied the effect of changing the internal CT scanner settings on the accuracy of the model reconstruction. The segmentation of the bone (pig tibia) was accomplished with a 3D Slicer and a threshold. Furthermore, the influence on bone geometry accuracy was evaluated using a 3D scanning model. Argüello et al. [14] presented a comparison of three tools: 3D Slicer, ITK-Snap, and InVesalius. Several methods, including threshold, growth from seeds, active contour, and manual segmentation, were used to rebuild vertebrae from CT images. Furthermore, a manual segmentation model was used as a reference model. According to the findings, growing from seeds with a 3D slicer was the best choice with 9.59% of volume error.

In summary, previous works can be divided into two categories. One of them focused on using images to make the 3D point cloud, while the other focused on using these images to rebuild the models using applications. However, the use of the threshold approach in both categories is a point of convergence in the majority of works. Besides, some studies used the region growth and active contour approaches. However, these approaches are sensitive to thin and poorly connected regions that are common in cancellous tissue. Furthermore, the kind of bone and its morphology, the intensity variance of the same tissues across slices, and image noise are some of the obstacles to obtaining an accurate segmentation. As a result, over- or incomplete segmentation occurs more frequently. Medical image reconstruction applications are no exception to this. Additionally, the segmentation process in these applications is dependent on user-defined threshold values or seed points. Moreover, these applications produce models that are more intricate and contain many holes. As a result, further processing is necessary to repair and simplify it and make it appropriate for implant design using other programs. All of these processes have some effect on the accuracy of the models. These obstacles are sufficient to lead to a complex and inaccurate model. To overcome these obstacles, we proposed a method that would create simple and accurate 3D models from CT images. The distant and near regions of the joints can be segmented using the method. Therefore, the method never increases or decreases the ROI. Furthermore, the proposed method aids in acquiring actual bone features by removing the remaining points that do not reflect the bones. Unlike reconstruction applications, the resulting 3D model does not require any extra processing procedures. Therefore, the model of the proposed method is suitable for designing joint replacement implants. In the subsequent section, the proposed method is discussed in detail.

### 3. Framework of the proposed method

The reverse engineering process includes phases like data acquisition, pre-processing data, segmentation, and computer-aided design (CAD) model building. 3D points-data representations of ordinary objects may be produced by doing discrete sampling utilizing 3D scans and 3D measurement devices [15]. However, because of the complexity of the morphology of human anatomy, particularly for tissue and organs, a standard technique is to acquire 2D medicinal slices of the human body like CT/MRI. Image-based modelling requires three main steps i) Image acquisition using CT or MRI. ii) Image processing, which would arrange and process the images to find ROI. iii) 3D reconstruction of the ROI. Lastly, a 3D model of the bone's surface is created using 2D medical images. For this purpose, we proposed a method to generate a precise 3D model of the bones using CT images. The method framework parts are shown in Fig. 3.

#### 3.1 Data acquisition

Data acquisition is the initial stage in the creation of 3D models. Furthermore, the quality of the data determines the quality of the models. MRI and CT are the two technologies that can be used to image bones quantitatively in 3D. CT and MRI can give precise information for measuring anatomical features in 3D. Due to the high precision that CT provides for bone morphology, it has become the standard for bone imaging for 3D model reconstruction, especially for the design of implants.

The obtained data are stored in the standard DICOM (Digital Imaging and Communications in Medicine) format independent of the scanning method. DICOM files contain a large amount of information and may be seen if the proper DICOM viewing software has been installed. DICOM data may also be simply converted to several photo formats.

#### 3.2 Extracting ROI

When analyzing items in images, it's important to separate the items of interest from the remainder of the image. This task is achievable by segmentation. Segmentation is the process of separating an original photo into smaller regions that share characteristics like brightness, intensity, and color [16]. The process of segmentation of the bone from CT slices is a complicated one due to the variance of bone tissue intensity across slices. Furthermore, flesh or soft tissues surrounded by bone tissue takes up the

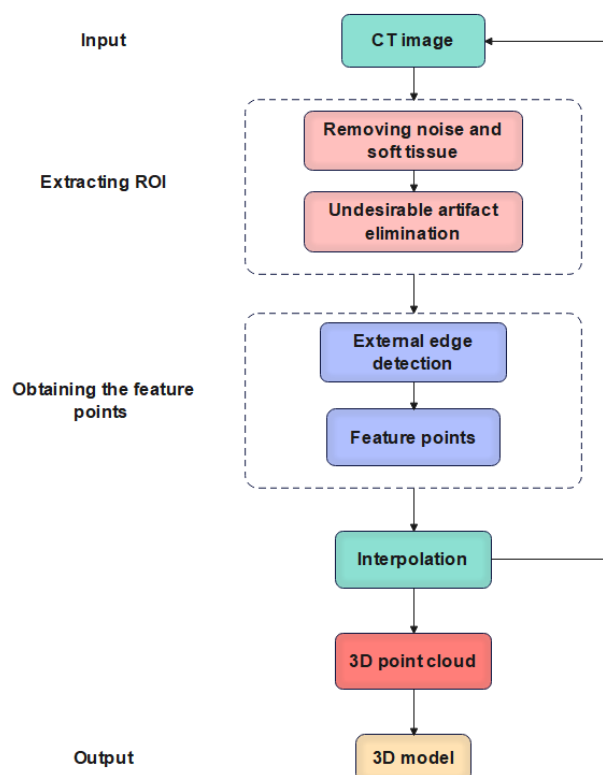


Figure. 3 Flowchart of the proposed method

majority of the CT image. Therefore, the goal of segmentation in the current stage is to isolate the target bone from its surroundings in a group of clinical CT slices. According to the literature, the threshold-based approach is commonly used to highlight the ROI in images. However, the thinner and fuzzy regions that are common in bone tissue have a detrimental effect on the results achieved using the conventional thresholding approach. The region-growing method is rapid and can conduct good segmentations of regions with similar attributes but isolated spatially. However, structures may be misconnected within the presence of noise and partial volume effects. Furthermore, the seed point is determined by manual interaction. Therefore, this approach frequently fails when applied to segment complex shapes such as long bones. Moreover, these techniques affect ROI quality. As a result, some of the bone's features may be missing. Additionally, when creating 3D models, the precision of the model is directly related to the image segmentation quality. The most difficult problem, in this case, is removing unwanted areas of the image without affecting the ROI.

In this section, eliminating soft tissues from CT images to extract ROI is done by using the proposed approach in [17]. This approach relies on histogram modelling and contrast stretching. Additionally, it

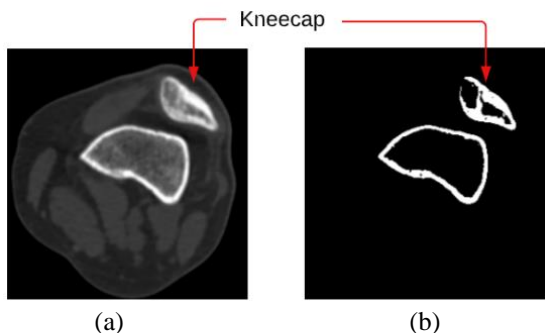


Figure. 4 CT slice: (a) Raw slice and (b) Slice after filtering

employs one of the intensity transformation methods to improve contrast. It is responsible for enhancing contrast by dispersing intensity values across a large range. This approach can eliminate unwanted flesh from an image without affecting the ROI. Besides, it enhances bone tissue in a simple and precise method. Moreover, it is superior to conventional segmentation techniques like thresholding, region-growing, and active contour. For these reasons, it is used at the current stage. The outcome of this approach is represented in Fig. 4.

### 3.3 Obtaining the feature points

After completing the second stage, the image consists of bone tissue and background. A pixel is considered to be on the border of bone tissue if at least one of its four linked neighbors has a value of zero. The method shown in Fig. 5 is used to extract the boundary pixels. Following that, the critical point (termed feature point) of the human bone tissue is recovered by converting border pixels to 2D coordinates in mm. On the right-hand side of Fig. 6, it is visible that the extracted feature points are accurate. The feature points are shown only on the right aspect of Fig. 6, while the non-feature points are removed. According to the results, the bone model's main shape is accurately represented by the feature points. This demonstrates the validity of the proposed method.

### 3.4 Interpolation

Interpolation is the next stage. The interpolation happens between two points. In numerical techniques, there are several interpolation methods, including linear, quadratic, and cubic interpolation. A linear interpolation approach ensures the correct answer at the interpolation point but excludes the derivative value of the interpolating function at that point. It is probable to generate crease errors during the bone development procedure; that is, borders are

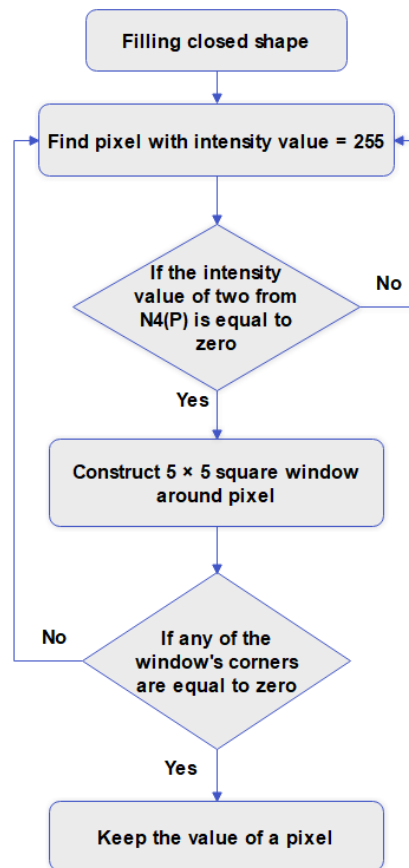


Figure. 5 Flowchart for detection of the external edge's pixel

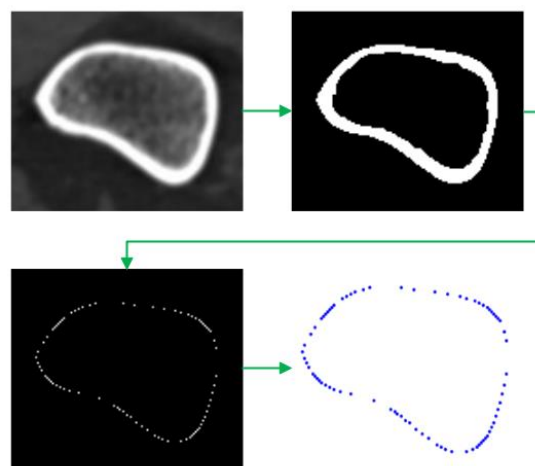


Figure. 6 Extraction of the feature points

too evident, and the view isn't realistic, particularly when producing bump textures. Since quadratic interpolation lacks a second derivative, it is unable to describe a curve with an inflection point. Therefore, cubic interpolation is commonly used in interpolation applications that need a smooth function passing across a specific collection of data points [18]. Not only does cubic interpolation give the right value at the node, but it also delivers the correct value for the



node's derivatives. Utilizing cubic interpolation ensures that the derivative of a function is the same at each interpolation node, making the result of interpolation smoother. So, the proposed method for interpolating the bone's feature points uses the cubic interpolation method.

In summary, the cubic spline is a series of cubic functions in a near period  $[x_{j-1}, x_j], j = 1, 2, 3, \dots, N$  amongst  $N$  data points. If  $N$  represents the total of points, the cubic spline function  $F(x)$  is given as [19, 20]:

$$F(x) = \begin{cases} f_0(x), & x \in [x_0, x_1] \\ \vdots \\ f_j(x), & x \in [x_{j-1}, x_j] \\ \vdots \\ f_{N-1}(x), & x \in [x_{N-1}, x_N] \end{cases} \quad (1)$$

Where  $f(x)$  is the cubic type function for  $j = 1, 2, 3, \dots, N-1$ .

The most general way to write a cubic spline is like this:

$$f_j(x) = a_j + b_j(x - x_j) + c_j(x - x_j)^2 + d_j(x - x_j)^3, j = 1, 2, 3, \dots, N - 1 \quad (2)$$

The result of substituting the beginning point for spline in Eq. (2) is:

$$y_j = f_j(x) = a_j, j = 1, 2, 3, \dots, N - 1 \quad (3)$$

Therefore, Eq. (2) can be rewritten as follows:

$$f_j(x) = y_j + b_j(x - x_j) + c_j(x - x_j)^2 + d_j(x - x_j)^3, j = 1, 2, 3, \dots, N - 1 \quad (4)$$

Where,  $b_j, c_j,$  and  $d_j$  are unidentified constants, and  $3(N-1)$  is the total number of constants. Conditions are given for determining the value of all unknown constants:

$$f_j(x_j) = y_j, \text{ and } f_j(x_{j+1}) = y_{j+1}, \text{ for } 1 \leq j \leq N - 1 \quad (5)$$

$$f'_{j-1}(x_j) = f'_j(x_j), \text{ for } 2 \leq j \leq N - 1 \quad (6)$$

$$f''_{j-1}(x_j) = f''_j(x_j), \text{ for } 2 \leq j \leq N - 1 \quad (7)$$

Here, the overall number of conditions is  $3N - 5$ :

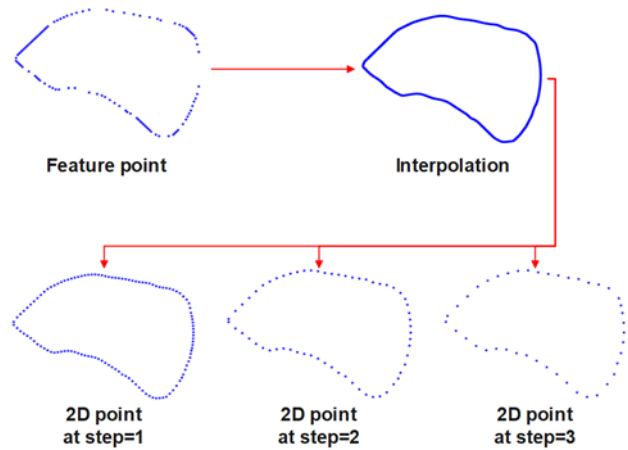


Figure. 7 The step's effect on the point cloud

For determining the values of all  $3N-3$  undetermined constants in Eq. (4), there is a need for two more conditions called cubic splines-boundary conditions. In this study, the conditions of the natural spline described below are used:

$$f''_0(x_0) = f''_{N-1}(x_N) = 0 \quad (8)$$

The above relations are linear, with unknown constant coefficients. So, solving splines is as easy as solving a set of linear algebraic equations.

### 3.5 3D point cloud creation

A 3D point cloud is a set of data points organized in a 3D coordinate system. These data points are typically described by X, Y, and Z coordinates, and are considerably used to describe an object's outer surface. By utilizing the proper tools and technology, 3D point cloud data may be produced from a range of data sources, such as laser scans, pictures, and videos [21]. Our study focused on CT images taken of the femur near the knee joint. A total of 285 slices are obtained, each measuring 0.6 mm in thickness (the distance between two adjacent slices). Feature points are collected from the slice and then interpolated. Next, the appropriate step is chosen to generate a new 2D coordinate. This process is repeated for each slice. As a result, a 3D point cloud is created. The efficiency of the point cloud depends upon the input feature points, which should be independent of noise and soft tissue. The proposed method provides fascinating control over the number of points in the cloud by adjusting the step, as seen in Fig. 7. Setting a step value aids in the acquisition of a homogeneous 3D point cloud. Since the slice thickness is 0.6 mm, the step is set to 0.6 to ensure that the distribution of points in the cloud is homogeneous. When a homogeneous point cloud is used, the triangulation of

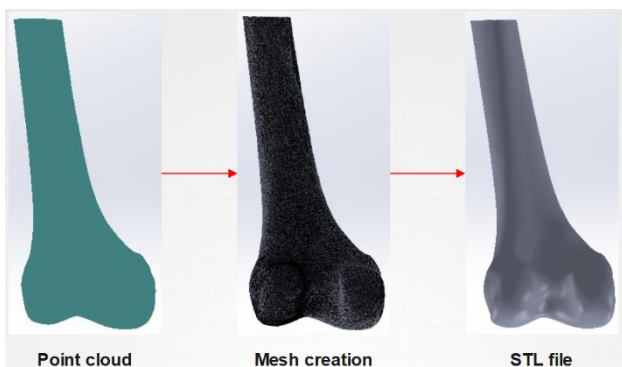


Figure. 8 The reconstruction process of the femur

the meshing is improved, and the file size gets smaller [22].

### 3.6 Reconstructing the 3D model

The process of reconstructing a 3D representation of an object from scanned data is referred to as 3D model reconstruction. In general, the reconstruction approach may be roughly categorized into two groups: surface reconstruction and volumetric reconstruction. However, surface models are better for the 3D representation of bone structures. The simplest method of surface representation from a point cloud is the triangulation method. The triangulation technique transforms a collection of points into a regular polygonal mesh. A polygonal surface model is a mesh made up of thousands or millions of linked triangles. Obviously, smaller triangular facets provide a smoother surface but raise the file size.

Through the use of RhinoCAM 2018's Mesh, the generated point cloud can be reconstructed into a 3D model. Following the mesh construction process, the mesh is re-meshed to make it smoother. Furthermore, the appropriate thickness is achieved by the offset mesh. Finally, the configuration is exported as a "Standard Triangulation Language" STL file. The thickness was calculated by taking the last slice and averaging its thickness. As a result, the femur entity model is created. These procedures are depicted in Fig. 8.

## 4. Results and discussion

### 4.1 Feature points

The feature point extraction using Sobel, Canny, and the proposed method is depicted in Fig. 9. The Sobel method used in [6] and the Canny method show the bone boundaries as sharp edges, straight lines, and perpendicular angles. These angles and lines are the natural results of the image's construction. Therefore,

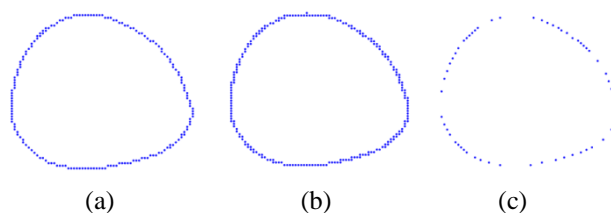


Figure. 9 Obtaining the feature points: (a) Sobel method, (b) Canny method, and (c) Proposed method



Figure. 10 The femur model

they do not represent the geometry of the bone tissues. Unlike Sobel [6] and Canny's method, the proposed method contributes to removing these angles and straight lines when extracting bone features from the filtered images. Consequently, using the proposed method gives only points that represent actual bone features, while eliminating the remainder of the points. Furthermore, this increases the interpolation's flexibility and smoothness. This is a strong indication of the performance of the proposed method.

### 4.2 3D model

#### 4.2.1. 3D Printing

The model was prepared for 3D printing once it had been saved in STL format. 3D printing on a low budget was easy with the Ender 5 Pro. It is a fused deposition modeling (FDM) printer with a new and enhanced Z-axis and dual Y-axis control system, making it easier to print. The nozzle diameter is 0.4 mm, the extrusion temperature is 200 °C, and the default printing speed is 40 mm/s. The layer's thickness has been set to 0.16 mm to ensure the surface's quality and dimensional precision. The 3D printer has a maximum precision of 0.1 mm. The 3D model was created using polylactic acid (PLA) filament. The femur model is shown in Fig. 10.

#### 4.2.2. Results comparison

In order to verify the proposed method's performance, an open-source application like 3D

Slicer is used to compare the results. The application employs a user-interactive technique to rapidly and semi-automatically generate a 3D model from medical images. Because of this, several works, including [10, 11, 13], have used it to create basic 3D models. Although the processing procedures for these studies differ. However, when using 3D Slicer to create the basic 3D model from CT images, the accuracy of the final 3D model is dependent on the accuracy of the basic model (3D Slicer's model before repairing holes and simplifying). Therefore, a comparison has been made with these studies in this section. Furthermore, similar results were recorded to the results of some studies, like [9] and [14].

A threshold method was used to segment the bones. The linear attenuation coefficient for bones has been chosen as the threshold value at this point. It is made up of 300 Hounsfield Units (HU). This value corresponds to the cortical bone area as well as the Cancellous bone to some extent. Consequently, only the middle part of the femur was successfully reconstructed, while the end part (near the joint) reconstruction was incomplete. Image segmentation errors are represented in red in Fig. 11.

A comparison of the 3D model from the proposed method and 3D Slicer is depicted in Fig. 12. The model of 3D Slicer contains many errors and holes in the model structure near the joint. Setting the threshold value for ROI extraction causes these issues. To fix these mistakes, other tools like MeshLab and Blender must be used [9]. This means that more processing steps must be done. However, further processing procedures reduce the accuracy of the 3D model. Furthermore, the techniques for repairing such models are not simple due to the model's internal complexity. This complexity occurs due to the volumetric reconstruction of the ROI. As a result, it requires more time and a more powerful CPU. Additionally, reducing the threshold value to select the regions near the joint results in a model with fewer holes. This procedure causes over-segmentation, resulting in the creation of a model larger in size than the real bone. Fig. 13 depicts the influence of the threshold on the model's accuracy. The right side of Fig. 13 represents the model resulting from a segmentation with a 300 HU threshold. While the model on the left has a threshold value of 400 HU. The effect is visible in the precision of the model dimensions. All segmentation methods in open-source applications have some degree of inaccuracy [14]. Unlike 3D Slicer's model, the proposed method's model is completer and more accurate. Moreover, it is more compatible with real bone. Additionally, the 3D model is of less

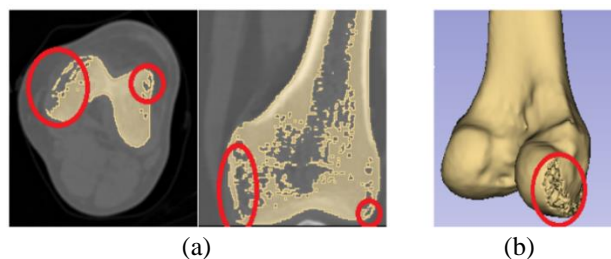


Figure. 11 3D Slicer procedures: (a) Errors in the femur's segmentation near the joint and (b) Holes in the femur model at the joint

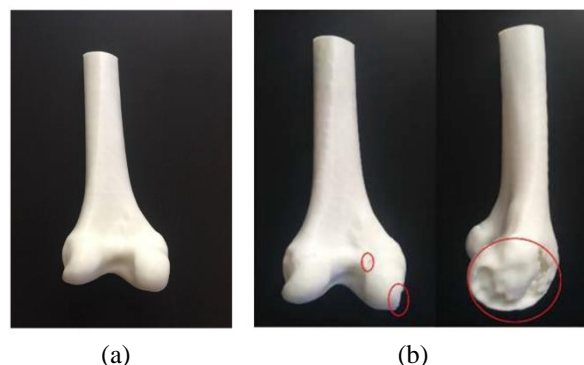


Figure. 12 The proposed method vs. 3D Slicer: (a) Proposed method and (b) 3D Slicer

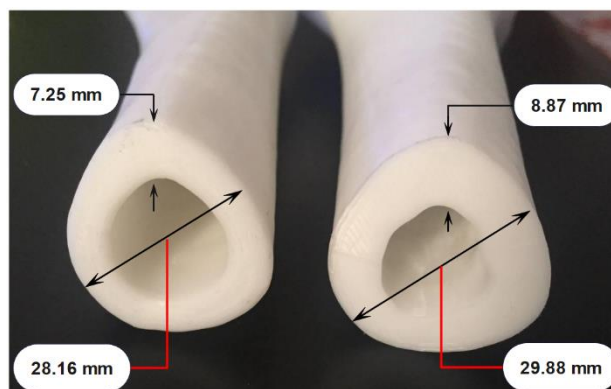


Figure. 13 The effect of the threshold on the model's accuracy in 3D Slicer

complexity and consumes less time during the printer process. For these reasons, the model is suitable for designing implants.

## 4.3 Evaluating accuracy

### 4.3.1. Reference model

A reference model is necessary to evaluate the accuracy and quality of the proposed method's results. Therefore, the bone of a sheep was utilized for this purpose. The bone was scanned using CT equipment, with a thickness of 0.6 mm. The pictures taken during the experiment are presented in Fig. 14. Following the CT scan, soft tissues and flesh were removed from



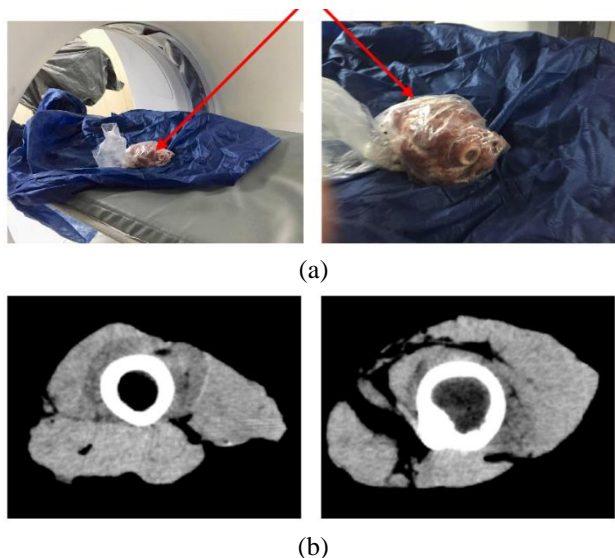


Figure. 14 Scanning of sheep bone: (a) Preparing for scanning and (b) CT images after scanning

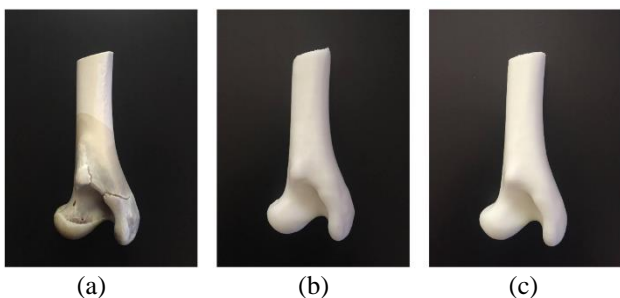


Figure. 15 Sheep bone models: (a) Reference model, (b) 3D Slicer's model, and (c) Proposed method's model

the bone using dissection. Although soft tissues may be removed from bones utilizing boiling or chemical processes, these approaches were not employed because they may affect the bone's surface geometry. During the surgery, caution was taken to avoid damaging the bone's surface. After soft tissue had been completely removed, the bone was dried in sun for four hours. Consequently, the reference model represented in Fig. 15 (a) was established.

The proposed method and 3D Slicer were used to produce 3D models of a sheep's bone. Unlike human bones, defects did not develop during the reconstruction process in the 3D Slicer. The low density of soft tissues around the bones is responsible for this. Additionally, there is a difference in X-ray attenuation for cancellous bones. The models were printed with the same 3D printer and parameters. Fig. 15 displays the sheep bone models.

#### 4.3.2. Comparison of models

A coordinate measuring machine (CMM) can be used to assess the models. Unfortunately, the CMM

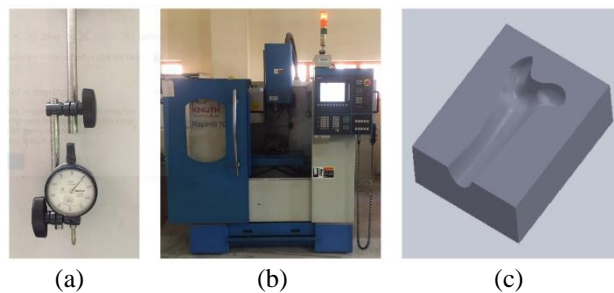


Figure. 16 Tools used: (a) Dial Indicator, (b) CNC milling machine, and (c) A mold

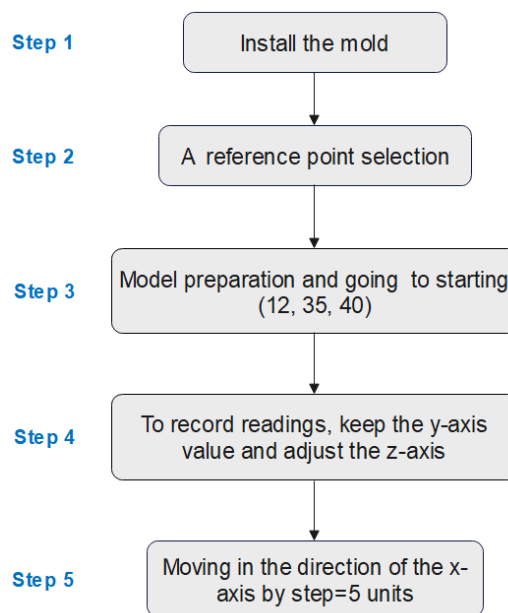


Figure. 17 Measurement steps

is not available at our university at present. Therefore, the testing was carried out using a computer numerical control (CNC) milling machine with the Dial Indicator. Because of the complex geometric shape of the bones, there was a requirement to design and manufacture a mold to appropriately install models on a machine table. The tools that were utilized are seen in Fig. 16.

During the test, the mold was permanently fixed on the machine table. A dial indicator was used as a contact probe to choose the reference point and reset the machine's coordinates to it. The measuring process was then started by moving to point (12,35,40). This point represents the starting point for measuring all readings. Fig. 17 illustrates the measurement steps. The final steps included fixing the Y-axis at 35 units and moving the X-axis with a fixed step of 5 units to obtain the readings listed in Table 1. The readings were taken by adjusting the Z-axis by observing the Dial Indicator. All readings relative to the reference point were acquired from the control screen of the machine.

Table 1. Measurements of the models (the unit is mm)

Reference model			3D Slicer			Proposed method		
X	Y	Z	X	Y	Z	X	Y	Z
12	35	11.73	12	35	13.22	12	35	12.01
7	35	11.75	7	35	13.7	7	35	12.07
2	35	11.85	2	35	13.75	2	35	12.13
-3	35	12.14	-3	35	13.93	-3	35	12.53
-8	22	12.55	-8	35	14.29	-8	35	12.87
-13	35	13.12	-13	35	14.79	-13	35	13.31
-18	35	13.55	-18	35	15.1	-18	35	13.72
-23	35	14.02	-23	35	15.48	-23	35	14.14
-28	35	14.84	-28	35	16.17	-28	35	14.88
-33	35	15.92	-33	35	17.1	-33	35	15.94

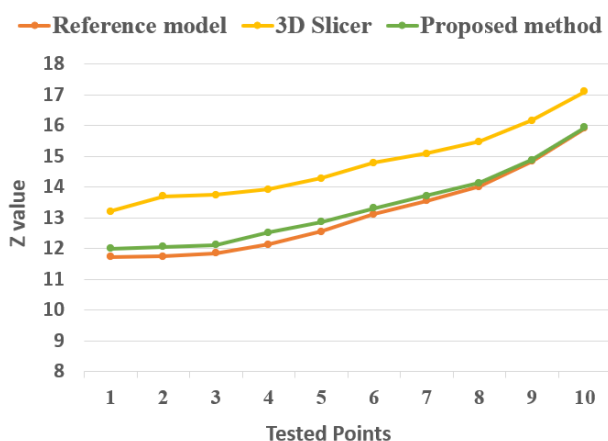


Figure. 18 Comparison between the models

According to Fig. 18, the proposed method's model is closer to the reference model and 10.596% superior to the 3D Slicer model. On the other hand, the error percentage between the proposed method and the actual bone was approximately 1.62%. While the percentage of error between the 3D Slicer and the actual bone was around 12.216%. The following reasons possibly account for the variance between the proposed method and the reference model: i) the printer's quality, ii) the triangulation error, and iii) the measuring process's accuracy. However, the proposed method provides promising findings.

## 5. Conclusion

This paper presented a novel method for 3D model reconstruction from CT images. Initially, soft tissues are removed from the images using a simple and precise technique. Next, a simple method has been devised to extract bone features. Our method for obtaining bone features is more effective than conventional edge detection methods. By using interpolation, we were able to make the point cloud's distribution of points more homogeneous. This improves the process of reconstructing 3D models. In contrast to other techniques described in the literature, the models of the proposed method are more accurate, less complex, and do not require additional processing steps. To comment on the validity and performance of the proposed method, it was tested on CT stacks of the femur bone and sheep bone. We compared our findings with real bone and achieved an accuracy of 98.38%. Furthermore, models were printed using a low-cost printer. However, the difference was obvious both visually and analytically. Consequently, the proposed method may be used to aid in designing joint replacement implants for patients before surgical intervention.

Besides, future works will concentrate on the following points: i) Segmenting the image and obtaining the ROI using deep learning. ii) Reconstruction of a 3D model from a point cloud using parametric surfaces like B-Spline or NURBS.

## Conflicts of interest

The authors advertise that they do not have any conflicts of interest.

## Author contributions

The methodology, data collection, implementation, and software have been done by the first author. Editing, work evaluation, and supervision are provided by the second and third authors.

## References

- [1] N. Archip, R. Rohling, V. Dessenne, P. J. Erard, and L. P. Nolte, "Anatomical structure modeling from medical images", *Comput. Methods Programs Biomed.*, Vol. 82, No. 3, pp. 203–215, 2006.
- [2] J. M. Edmund and T. Nyholm, "A review of substitute CT generation for MRI-only radiation therapy", *Radiat. Oncol.*, Vol. 12, No. 1, pp. 1–15, 2017.
- [3] M. A. Fuessinger, S. Schwarz, C. Cornelius, M. C. Metzger, E. Ellis, F. Probst, W. S. Hogg, M.

- Gass, and S. Schlager, "Planning of skull reconstruction based on a statistical shape model combined with geometric morphometrics", *Int. J. Comput. Assist. Radiol. Surg.*, Vol. 13, No. 4, pp. 519–529, 2018.
- [4] F. Paulano, J. J. Jiménez, and R. Pulido, "3D segmentation and labeling of fractured bone from CT images," *Vis. Comput.*, Vol. 30, No. 6–8, pp. 939–948, 2014.
- [5] R. Menaka, C. Chellamuthu, and R. Karthik, "Efficient 3D point cloud generation from medical images in frequency domain using discrete curvelet transform", *Eur. J. Sci. Res.*, Vol. 60, No. 2, pp. 305–315, 2011.
- [6] V. N. Chougule, A. V. Mulay, and B. B. Ahuja, "Three dimensional point cloud generations from CT scan images for bio-cad modeling", *Int. Conf. Addit. Manuf. Technol-AM2013*, p. 5, 2013.
- [7] S. Zhang, B. Jiang, H. Shi "Jawbone Segmentation with Trabecular Bone Preservation from Cone Beam CT Images", *Applied Sciences*, Vol. 12, p. 1556, 2022.
- [8] S. G. Izard, J. A. Méndez, P. R. Palomera, and F. J. G. Peñalvo, "Applications of Virtual and Augmented Reality in Biomedical Imaging", *Journal of Medical Systems*, Vol. 43, No. 4, pp. 1–5, 2019.
- [9] F. Osti, G. M. Santi, M. Neri, A. Liverani, L. Frizziero, S. Stilli, E. Maredi, P. Zarantonello, G. Gallone, S. Stallone, and G. Trisolino, "CT conversion workflow for intraoperative usage of bony models: From DICOM data to 3D printed models", *Appl. Sci.*, Vol. 9, No. 4, pp. 1–12, 2019.
- [10] N. I. Alawy and A. B. Abdulghafour, "The virtual surgery to reconstruct the mandible using digital images", In: *Proc. of 2nd International Conference On Materials Engineering & Science (IconMEAS 2019)*, p. 020163, 2020.
- [11] P. R. Masilamani, A. S. Muralidharan, and A. K. Dash, "Structural Analysis of Hip Joint from 3D model Generated from DICOM File using Slicer 3D", *Int. J. Innov. Sci. Res. Technol.*, Vol. 6, No. 12, pp. 130–133, 2021.
- [12] E. Soodmand, D. Kluess, P. A. Varady, R. Cichon, M. Schwarze, D. Gehweiler, F. Niemeyer, D. Pahr, and M. Woiczinski, "Interlaboratory comparison of femur surface reconstruction from CT data compared to reference optical 3D scan", *Biomed. Eng. Online*, Vol. 17, No. 1, pp. 1–10, 2018.
- [13] L. Puggelli, F. Uccheddu, Y. Volpe, R. Furferi, and D. Di Feo, "Accuracy assessment of CT-based 3D bone surface reconstruction", *Design Engineering and Manufacturing II, Springer International Publishing*, Cham, pp. 487–496, 2019.
- [14] D. Argüello, H. G. S. Acevedo, and O. A. G. Estrada, "Comparison of segmentation tools for structural analysis of bone tissues by finite elements", *Journal of Physics: Conference Series*, Vol. 1386, No. 1, p. 12113, 2019.
- [15] T. Liu, J. Gao, and Y. Zhao, "An approach to 3D building model retrieval based on topology structure and view feature", *IEEE Access*, Vol. 6, pp. 31685–31694, 2018.
- [16] N. Thein, T. B. Adji, K. Hamamoto, and H. A. Nugroho, "Automated False Positive Reduction and Feature Extraction of Kidney Stone Object in 3D CT Images", *Int. J. Intell. Eng. Syst.*, Vol. 12, No. 2, pp. 62–73, 2019, doi: 10.22266/ijies2019.0430.07.
- [17] D. D. Ruikar, K. C. Santosh, and R. S. Hegadi, "Automated Fractured Bone Segmentation and Labeling from CT Images", *J. Med. Syst.*, Vol. 43, No. 3, pp. 1–13, 2019.
- [18] G. Turk and J. F. O'Brien, "Modelling with implicit surfaces that interpolate", *ACM Trans. Graph.*, Vol. 21, No. 4, pp. 855–873, 2002.
- [19] K. Ansari and S. K. Sharma, "Ionospheric TEC variation based on GNSS data over the Arabian Peninsula and validation with the cubic spline interpolated GIM model", *Adv. Sp. Res.*, Vol. 68, No. 9, pp. 3814–3820, 2021.
- [20] T. Sauer, *Numerical Analysis, 3rd ed*, Pearson Education, Hoboken New Jersey, 2018.
- [21] Q. Wang and M. K. Kim, "Applications of 3D point cloud data in the construction industry: A fifteen-year review from 2004 to 2018", *Adv. Eng. Informatics*, Vol. 39, pp. 306–319, 2019.
- [22] B. R. Barbero and E. S. Ureta, "Comparative study of different digitization techniques and their accuracy", *CAD Comput. Aided Des.*, Vol. 43, No. 2, pp. 188–206, 2011.